Chemical Physics 399 (2012) 4–16

Contents lists available at SciVerse ScienceDirect

Chemical Physics

journal homepage: www.elsevier.com/locate/chemphys

ChemPhys Perspectives

Structure and dynamics of noble gas-halogen and noble gas ionic clusters: When theory meets experiment

J.A. Beswick [a,*], N. Halberstadt [a], K.C. Janda [b]

[a] Université de Toulouse, UPS, and CNRS, UM5589, Laboratoire Collisions, Agrégats, Réactivité, IRSAMC, F-31062 Toulouse, France
[b] Department of Chemistry and Institute of Surface and Interface Science, University of California at Irvine, Irvine, CA 92697-2025, United States

ARTICLE INFO

Article history:
Available online 17 June 2011

Keywords:
Van der Waals molecules
Ionic clusters
Fragmentation
Intramolecular vibrational redistribution
Vibrational and electronic predissociation

ABSTRACT

As part of this special issue in honor of Gerardo Delgado Barrio, we have reviewed the interplay between experimental and theoretical work on halogen and interhalogen diatomic molecule bonded to one or more noble gas atoms and also ionic clusters consisting of noble gas atoms. Although the Madrid group has worked on many theoretical issues, they have made particularly important contributions to these two topics. Delgado Barrio has often chosen topics for study for which close interactions between theorists and experimentalists are especially useful. During the historical span of the group, we have progressed from approximate models whose goal was to capture the essence of a process even if the details were impossible to reproduce, to an era in which theory is an equal partner with experiment, and, in fact, often provides a detailed understanding beyond that obtained from a careful analysis of state-of-the-art data.

1. Introduction

Atomic and molecular clusters are ideal model systems to study the evolution of characteristic properties from single molecules to the condensed phase. The hope is to find an explanation of macroscopic effects on a molecular scale, which is difficult to access in the condensed phase but can in principle be readily accessed by studying them as a function of cluster size. Fig. 1 illustrates an example of the goals of this type of research. The picture shows three bottles of molecular iodine, each containing a different solvent. The color of the iodine is very sensitive to the solvent properties. The shifts in the valence electronic spectrum of iodine are so substantial that the color changes are dramatic. One goal of this research field is to understand these color changes based on the details of the interaction between the iodine and the solvent molecules.

Intramolecular energy flow in molecular systems is one of the most basic processes in chemical dynamics. It determines for instance, the unimolecular reaction rates, intramolecular relaxation, and energy disposal in fragmentation. Van der Waals (vdW) clusters with one molecule (the chromophore) weakly bound to one or several rare-gas atoms are ideal prototypes for the study of these energy transfer processes. Since the molecule retains most of its individual properties, one can, under suitable conditions, excite the system with the excess energy localized in electronic, vibrational and/or rotational degrees of freedom of the chromophore and follow the energy disposal and redistribution in the cluster.

The study of energy acquisition and disposal in these systems is important for at least two reasons. On the one hand, it allows us to understand in detail very basic chemical processes such as bond breaking and energy relaxation. On the other hand, these systems are simple enough that they provide benchmarks for dynamicists to check the validity of their theoretical approaches, and for ab initionists to develop accurate techniques to determine from first principles the properties of intermolecular interactions. These in turn are important for applications to more complex systems such as larger clusters, molecules embedded in clathrates or rare gas matrices, and molecules in solution.

Ionic noble gas clusters are another type of system which are ideal for the study of fragmentation processes. Vertical ionization of a neutral van der Waals cluster usually gives the system sufficient vibrational energy to eject one or several noble gas atoms. The study of fragment mass distribution as a function of the cluster size provides crucial information on the dynamics of the fragmentation process. This is very important for the interpretation of mass spectrometry measurements, in which the ion mass distribution can be quite different from the initial neutral cluster one. In addition, the pathways of energy disposal in these systems: evaporation, fission, atom ejection, can be the initial steps for energy relaxation in condensed phase.

In this paper we review the work on van der Waals molecules formed with a halogen or interhalogen diatom (XY) bound to one or several noble gas atoms (Ng), and the work on the ionic clusters prepared by ionization of pure or mixed noble gas neutral clusters.

* Corresponding author.
E-mail address: beswick@irsamc.ups-tlse.fr (J.A. Beswick).

0301-0104/$ - see front matter © 2011 Elsevier B.V. All rights reserved.
doi:10.1016/j.chemphys.2011.05.026

Fig. 1. Iodine in cyclohexane, dichloromethane and water. Why are the colors so different? Could you guess which is which?

It is in this area where the Madrid group headed by Delgado-Barrio contributed actively over many years with theoretical work in close relationship with experiments. The paper is organized as follows. In Section 2 we discuss the work done on noble gas-halogen van der Waals dimers. In Section 3 the work on larger noble gas-halogen clusters are reviewed. Finally, Section 4 deals with the structure and dynamics of the noble gas ionic clusters.

2. Noble gas-halogen van der Waals dimers

It is now well known that for halogen molecules in the ground electronic state, noble gas atoms can stick on either end or in a *T-shaped* configuration perpendicular to the halogen bond (see for instance Ref. [1]). For the linear isomers, the van der Waals attraction is enhanced because the noble gas atom can approach the halogen atom somewhat closer due to the unoccupied σ^* orbital. The T-shaped isomer is favored by the interaction of the noble gas atom with two halogen atoms. These effects are remarkably well balanced, and often the two isomers have the same binding energy within experimental error. It is also somewhat remarkable for the He containing species that wide amplitude bending vibrations do not lead to interchange between the two isomers.

At the time of the above cited review [1] on noble gas-halogen dimers most of the *T-shaped* isomer structures had been measured, but there was still relatively little information available on the linear isomers. The linear isomers were actually the first to be discovered [2,3], but their existence was somewhat surprising from the very beginning. If they were true van der Waals molecules, one would expect the *T-shaped* geometry for which maximal contact can be obtained. When Levy and colleagues first obtained dynamics data for the noble gas-iodine species [4], the early theoretical treatments [5] assumed that the structures were linear. However, it soon became evident that these and the electronic spectra for these and other dimers incorporating homonuclear halogens corresponded to the T-shaped isomers [6]. There is little indication in the literature before 1993 that both linear and T-shaped isomers might exist for any other species.

The possible co-existence of both linear and T-shaped isomers was finally evident upon intense study of Ar···I_2. Levy's early work clearly indicated that Ar···I_2 has a relatively long-lived, most likely T-shaped isomer [7]. However, Herschbach [8], and especially Valentini [9], showed conclusively that there was also short-lived Ar···I_2 species for which the iodine constituent can be excited above its dissociation limit and yet survive. This was dubbed the *one atom* cage effect. In a careful study of absolute absorptivity, Klemperer [10] showed that the cage effect arose from a continuous spectrum superimposed on the discrete T-shaped features observed by Levy's group. It became evident that this continuum is due to the quickly dissociating linear isomer. About the same time, ab initio theory became reliable enough that a complete surface could be calculated and bound vibrational levels obtained for both the linear and T-shaped isomers of Ar···Cl_2 [11].

Over the past 8 years the group of Loomis has made an intensive study for the co-existence of multiple Ng···X_2 isomers [12]. They first confirmed the existence of both isomers for He···ICl [13]. In this case, the linear isomer also has discrete bands because the vibrational energy transfer rate is limited by the small amplitude motion of the heavy iodine atom. That the linear isomer is the more stable was determined by studying the band intensities as a function of distance from the nozzle [14]. This ingenious use of supersonic cooling enabled the Loomis group to measure the relative binding energy for the two isomers of He···ICl [15], Ne···ICl [16], He···Br_2 [20], and He···I_2 [21]. As may be expected, at least in retrospect, for the ICl species the linear isomer is significantly more stable than the T-shaped one. For the homonuclear halogens the two isomers have very similar binding energies even though the linear well is the deeper one. This is due to significantly higher zero-point energy for the linear isomer.

With the development of ab initio electronic structure calculations, it became possible to reliably calculate the ground electronic state surfaces for Ng···XY dimers. The group of Delgado-Barrio has been especially active in this regard and has calculated state-of-the-art potentials for Ng···I_2 [22–24], Ng···Br_2 [25–29], Ng···ICl, [30,31], and Ng···ClF [32,33]. Obtaining ab initio surfaces for the excited states is more complicated since the standard programs do not incorporate the proper cylindrical symmetry of the halogen moiety, nor do they treat the spin–orbit interaction in a transparent way. One approach to this difficulty is to average the two limiting geometries with respect to the planar π orbitals [34]. The Delgado-Barrio group has made significant contributions to this problem [35,36,39].

2.1. Direct vibrational predissociation

In a triatomic complex formed with a diatomic molecule (XY) and a noble gas atom (Ng), the vibrational frequency of the diatom is much higher than the van der Waals mode frequencies, providing a clear separation between these two degrees of freedom. In a time-dependent picture one can then define an initial excited state of the complex in which the energy is localized in the vibration of the diatomic molecule. Since this excess energy is usually much larger than the van der Waals binding energy, energy redistribution within the complex will eventually break the van der Waals bond. This is a clear example of a vibrational predissociation (VP) process of the type

$$\mathrm{Ng}\cdots\mathrm{XY}(v) \rightarrow \mathrm{Ng} + \mathrm{XY}(v' < v) + \epsilon \qquad (1)$$

where v is the quantum number associated to the initial vibrational level of XY, v' its final vibrational level after fragmentation, and ϵ, the energy released into relative translational motion.

This field developed from the pioneering experimental work of Levy and collaborators in Chicago [4,40,41,7]. With iodine as the chromophore co-expanded with helium in a supersonic beam, they were able to form the He···I_2 complex at very low vibrational and rotational temperatures. By laser excitation fluorescence techniques in the region of the B ← X electronic transition they studied the VP process for different vibrational levels of the B state. Lifetimes and vibrational state distributions were determined for a large number of vibrational states. This first experiments were followed by an intense, both theoretical and experimental, activity on many other complexes and larger clusters [1]. The most important finding is that the fragmentation process is quite selective and that the simplest statistical theories of unimolecular reaction rate are not adequate to describe these systems. In fact, the application of Rice–Ramsberger–Kassel–Marcus (RRKM) theory to the very simple reaction (1) leads to about a l000-fold overestimate of the rate [42].

2.1.1. Analytical model for direct VP

Beswick and Jortner [5,43,44] provided an analytical calculation of the vibrational predissociation of Ng···XY vdW complexes, based on a simplistic model with the system constrained to be in a collinear configuration Ng–X–Y and the interaction between the rare gas atom and the X atom described by a Morse potential. The vibrational predissociation rates were calculated using the Golden rule approximation and first order expansion of the vdW potential in terms of the XY vibrational mode. Furthermore, the process was assumed to be due to a direct coupling between the initial quasi-bound state and the final continua (direct vibrational predissociation).

The Hamiltonian was written as

$$-\frac{\hbar^2}{2\mu}\frac{\partial^2}{\partial r^2}-\frac{\hbar^2}{2m}\frac{\partial^2}{\partial R^2}+U(r)+V(R_{vdW}) \tag{2}$$

where $r = R_{XY}$ is the vibrational coordinate and μ the reduced mass of the XY diatom and

$$R = R_{vdW}+\gamma r;\quad \gamma = M_Y/(M_X+M_Y) \tag{3}$$

is the distance between Ng and the center of mass of XY. The reduced mass associated to R is $m = M_{Ng}(M_X+M_Y)/(M_{Ng}+M_X+M_Y)$. $U(r)$ is the potential for the isolated diatomic and $V(R_{vdW})$ is the van der Waals interaction which was expanded as

$$V(R_{vdW}) \equiv V(R-\gamma r) \simeq V_0(R)+V_0'(R)(r-r_0) \tag{4}$$

where $V_0(R) = V(R-\gamma\ r_0)$ and $V_0'(R) = (\partial V/\partial r)_{r_0}$ with r_0 being the equilibrium distance of XY.

Since the van der Waals interaction perturbs only slightly the diatomic molecule, zero-order wavefunctions were written as products of a function $\chi_v(r)$, solution of the free diatomic vibrational Hamiltonian

$$H_{XY} = -\frac{\hbar^2}{2\mu}\frac{\partial^2}{\partial r^2}+U(r) \tag{5}$$

with energy E_v and a solution of the van der Waals zero-order Hamiltonian

$$H^{(0)}_{Ng\cdots XY} = -\frac{\hbar^2}{2m}\frac{\partial^2}{\partial R^2}+V_0(R) \tag{6}$$

which has both discrete, $\phi_\ell(R)$, and continuum, $\phi_\epsilon(R)$, wavefunctions with energy $-\epsilon_\ell$ and ϵ with respect to the Ng + XY dissociation limit, respectively.

In the energy-resolved picture, the quasibound state

$$\psi_{v,\ell} = \chi_v(r)\phi_\ell(R) \tag{7}$$

can be considered as an isolated bound state coupled to a set of continua if its line width is small compared with the energy separation between vibrational levels. The coupling of this state by H to the continuum states

$$\psi_{v',\epsilon} = \chi_{v'}(r)\phi_\epsilon(R) \tag{8}$$

with $v' < v$ is responsible for vibrational predissociation, and the partial rate (resonance half-width) of each final state v' is given by the Golden rule formula

$$\Gamma_{v\to v'} = \pi\left|\left\langle\psi_{v,\ell}\right|\left(H-H_{XY}-H^{(0)}_{Ng\cdots XY}\right)\left|\psi_{v',\epsilon}\right\rangle\right|^2 \tag{9}$$

where from Eqs. (4)–(6), it follows that

$$H-H_{XY}-H^{(0)}_{Ng\cdots XY} = V_0'(R)(r-r_0) \tag{10}$$

In Eq. (9) the energy of the continuum wavefunction has to be taken equal to the one of the quasi-bound level. Hence,

$$\epsilon = E_v-\epsilon_\ell-E_{v'} \tag{11}$$

The total rate is given by $\Gamma_v = \sum_{v'}\Gamma_{v\to v'}$ and the lifetime is $\tau^{(v)} = \hbar/2\Gamma_v$. The probability of a given product vibrational level is then $P_{v'} = \Gamma_{v\to v'}/\Gamma_v$.

The introduction of $H-H_{XY}-H^{(0)}_{Ng\cdots XY}$ from Eq. (10) into Eq. (9) gives

$$\Gamma_{v\to v'} = \pi|\langle\chi_v|(r-r_0)|\chi_{v'}\rangle|^2|\langle\phi_\ell|V_0'|\phi_\epsilon\rangle|^2 \tag{12}$$

The $|\langle\chi_v|(r-r_0)|\chi_{v'}\rangle|^2$ factor yields a strong propensity rule $\Delta v \equiv v'-v = -1$. The last factor of Eq. (12) is an integral of a product of three functions (see Fig. 2): (a) the ground van der Waals state wave function, $\phi_\ell(R)$, which varies smoothly with R; (b) V_0', the derivative of the interaction potential with respect to r, which varies strongly with R in the repulsive region, goes to zero at R_e and is slightly negative for large R; and (c) the continuum function $\phi_\epsilon(R)$, which has a maximum near the classical turning point of the repulsive wall of the v' potential and oscillates at large R as a de Broglie wave. Since the continuum function oscillates rapidly in the region where the bound state wave function is significantly different from zero, then the integral tends to cancel out. Indeed, it was shown that the rate can be approximated by

$$\Gamma_{v\to v'=v-1} \propto ve^{-\pi\theta(v)} \tag{13}$$

with $\theta(v)$ depending on the XY vibrational frequency ω as

$$\theta(v) \propto \sqrt{\hbar\omega-\epsilon_\ell-\hbar\omega\chi v} \tag{14}$$

This result neatly describes the non-linear dependence on v of the vibrational predissociation rates.

2.1.2. Numerical calculations

Although the analytical model reviewed above qualitatively describes the main features of rates and final state vibrational distributions for direct VP in systems such as He···I_2, the collinear model is not appropriate for many systems which have T-shaped or bent equilibrium configurations. Moreover, the effects of rotations are not included. Also the production of $v' < v-1$ channels are non-negligible in many systems and even for a system such as He···I_2 for initial states where the $v-1$ channel is closed ($v > 50$) the predissociation into the $v-2$ channel is not direct but actually proceeds via excited van der Waals bound states of the $v-1$ channel, i.e., there is IVR (intramolecular vibrational redistribu-

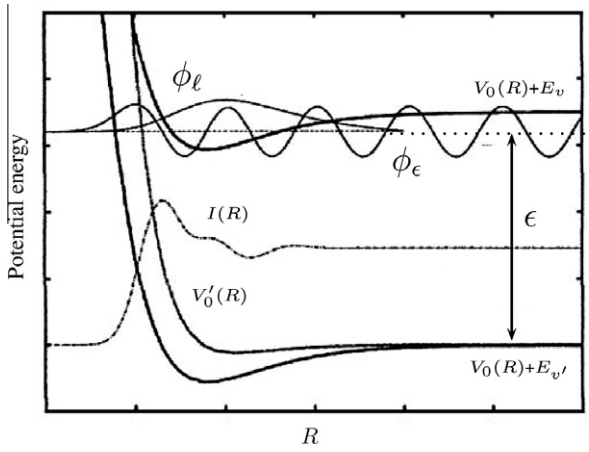

Fig. 2. The Golden rule zero-order picture and the main factors giving the vibrational predissociation rates. The discrete $\phi_\ell(R)$ wave function is a bound state of the van der Waals potential V_0+E_v channel. The continuum wavefunction $\phi_\epsilon(R)$ is a dissociative state with final kinetic energy ϵ of the van der Waals potential $V_0+E_{v'}$ channel. The coupling operator is given by $V_0'(R)$, the derivative with respect to r of the van der Waals interaction. Finally $I(R)$ is the integral of the product $\phi_\ell V_0'\phi_\epsilon$ from 0 to R. For large R, $I \to \langle\phi_\ell|V_0'|\phi_\epsilon\rangle$.

tion) prior to dissociation. Thus more elaborate calculations had to be performed using realistic potentials, including all degrees of freedom, and treating the dynamics beyond the Golden rule approximation. Since analytical expressions are no longer available for these more complex problems, it is necessary to resort to numerical integration of the equations of motion. With that objective in mind, several groups conducted a series of quantum studies of VP in halogen and interhalogen molecules bound to a rare gas atom.

He···I_2 dimers. The first of such calculations was conducted by Delgado-Barrio and collaborators on He···I_2 using a more realistic T-shaped model potential [45]. The close-coupling equations for nuclear motion were solved by scattering techniques and the vibrational predissociation rates were related to the widths of the resulting resonances. The superlinear theoretical dependence of the vibrational predissociation rates on the excess vibrational energy of the molecular I_2 bond were in good agreement with the experimental data of Levy and coworkers,

$$\Gamma_v = 0.55510^{-4} v^2 + 0.17410^{-4} v^3 \ (\mathrm{cm}^{-1}) \quad \text{for} \quad 12 \leqslant v \leqslant 26. \tag{15}$$

The relative contribution of intramolecular and of intermolecular terms to this superlinear dependence was elucidated, demonstrating the effects of the anharmonicity of the molecular bond on the intramolecular dynamics.

The effect of rotations on VP of He···I_2 was then studied by Delgado-Barrio and Beswick [46,47], using a method closely related to the *rotational infinite order sudden approximation* of scattering theory. The He···I_2 molecule, with its small rotational constant, constitutes a suitable system for the application of this approximation. Final rotational distributions for the I_2 fragment were obtained. The distributions showed very little rotational excitation and the fraction of the available energy going to rotational energy of the I_2 fragment was small compared with the energy going to translational motion. It was therefore concluded that vibrational predissociation in the He···I_2 complex is essentially a pure half-collision V-T process, i.e., a direct transfer from vibrational to translational motion. Similar calculations on Ne···I_2 [48,49], reached essentially the same conclusions.

After these first studies, several more accurate and detailed quantum close-coupling calculations of pure VP in He···I_2 have been conducted by the Madrid team [50–52] in combination with the determination of new ab initio potential energy surfaces [23,53,24,54,36]. In Ref. [24] for instance, three-dimensional quantum mechanical calculations of He···I_2(B) state were performed using a potential energy surface accurately fitted to unrestricted open-shell coupled cluster ab initio data. A Lanczos iterative method with an optimized complex absorbing potential was used to determine energies and lifetimes of the vibrationally predissociating He···I_2(B, $v \leqslant 26$) states. The calculated predissociating state energies agree with experimental results within 0.5 cm^{-1}. This agreement is remarkable since there was no adjustment of the PES. The lifetimes on the other hand, highly sensitive to subtle details of the potential energy surfaces such as anisotropy, are a factor of 1.5 larger than the available experimental data.

Ng···Cl_2 dimers. Although the optical transitions for Cl_2 are much weaker than those of I_2, the lighter atoms allow for much better state resolution using the pump–probe techniques introduced by Lester and her group [55]. The first detailed experiments on Cl_2 complexes were conducted by the Janda group on Ne···Cl_2. This allowed for detailed comparisons between theory and experiments. Using empirical potentials Halberstadt et al. [37] conducted quantum close-coupling calculations on this system and found good agreement for lifetimes as well as final state vibrational and rotational distributions. Similar studies have been conducted for He···Cl_2 [38], with the same level of agreement.

Because it is the lightest noble gas-halogen species for which optical spectra can be obtained, the He···Cl_2 molecule has been studied with better experimental resolution and theoretical precision than the other species [38]. For example, product rotational state distributions for the $\Delta v = -1$, -2, and -3 dissociation channels of the He···Cl_2 B state, for initial vibrational levels between $v = 6$ and $v = 23$, were obtained. Several interesting phenomena were observed. The Cl_2 final rotational state distributions were distinctly bimodal, with one peak at $j = 2$ and a second peak at $j = 8$ and 10, and the rotational distributions are remarkably independent of Δv, even though the total product kinetic energy varies from 115 cm^{-1} for $\Delta v = -1$ to over 400 cm^{-1} for $\Delta v = -3$. The extra energy release for $\Delta v > 1$ mostly goes into the translational degrees of freedom of the products. These results were born out by the close-coupling calculations [38] and the shape of the rotational distribution was interpreted as due to a combination of a rotational rainbow effect and quantum interference.

Also, ab initio calculations of the potential energy surface for noble gas interactions with Cl_2 molecules are more reliable than those for I_2. Hence early ab initio calculations already gave results that were of the same quality level as the atom–atom potentials [57,34,58]. In addition, they showed the existence of a collinear minimum that could not be present in the empirical potentials used (see below).

In general, the data for Ne···Cl_2 [56,59] are analogous to those for He···Cl_2. Although the rate of vibrational predissociation changes rapidly with initial vibrational level, $\tau = 258 \pm 42$ ps for $v = 9$, and $\tau = 33 \pm 2$ ps for $v = 13$, the rotational distributions change relatively little with v. Distinct bimodal structure is observed for the $\Delta v = -1$ predissociation channel from low initial vibrational levels ($6 < v < 11$), but this is washed out both for higher vibrational levels and for the $\Delta v = -2$ channel. The rotational distributions for $\Delta v = -1$ and -2 relaxation are surprisingly similar, given that the product kinetic energy more than doubles for $\Delta v = -2$. The rotational distributions terminate abruptly at high j. This allowed for the bond energy of Ne···Cl_2 to be measured precisely and unambiguously. Also, excitation spectra originating in the $v = 1$ level of the X state were observed. These effects have also been studied theoretically by quantum close-coupling calculations [60,61].

Ng···Br_2. He···Br_2 is another triatomic complex which has been studied in detail both experimentally [17–20] and theoretically [62–69,25,26,28,35,70]. For low to intermediate v, good agreement with most of the data (spectral shifts, lifetimes, average structures, average product energies) was achieved. The closing of the $\Delta v = -1$ channel at $v = 44$ and the binding energy at that vibrational channel were successfully reproduced, although calculated and experimental blueshifts and linewidths were not in such good agreement in the $v > 38$ range. For these high v excitations, fragmentation cross sections exhibit complicated structures indicating strong interactions among different quasibound states. In addition, interesting threshold and intramolecular energy redistribution effects were predicted. The closing of the $\Delta v = -1$ channel was found to be a gradual process where different dynamical regimes can be investigated in detail. It was shown that energy in the He···Br_2(B, $v = 45$) quasibound state may be internally redistributed exciting van der Waals modes at the expense of the bromine excitation (IVR mechanism, see below) prior to dissociation. Such mechanisms were more deeply studied by means of the stabilization method, which works with square-integrable wave functions and is an appropriate approach to perform quasibound state analysis. Stabilization total cross sections compare fairly well with close-coupling ones, where the proper asymptotic behavior of the continuum wave functions is taken into account. By inspection of the quasibound state wave functions, it was seen that energy is

redistributed to several excited states belonging to the $v-1$ manifold. In addition, it was shown that such excited states also carry oscillator strength in the transition from the ground electronic state and thus interference effects in the excitation process are significant. He···Br_2 near the halogen dissociation limit is found to be a rather strongly coupled system where the quasibound states involved can only approximately be assigned to quantum numbers corresponding to interhalogen and van der Waals vibrational excitations.

Pump–probe spectra of He···Br_2 in vibrational states $v=10$ and 39 through 48 of the B electronic state were reported and the fragment rotational distributions from vibrational predissociation of the cluster were extracted from the measured $E\left(0_g^+\right) \leftarrow B(^3\Pi_{0u})$ spectra of Br_2 [67]. The experimental results were compared to theoretical calculations on the $B \leftarrow X$ spectra using atom–atom model potentials and performing a thermal average over transitions that contribute to the net excitation. Very good agreement between experiment and theory is obtained, except in the region of $v=44$, where the $\Delta v=-1$ channel closes, and in the region of $v=48$ where the $\Delta v=-2$ channel closes. For $v=43$, and $v=44$, the agreement is less satisfactory because the dynamics are extremely sensitive to details of the potential energy surface due to threshold effects associated with the $\Delta v=-1$ channel closing. Similar sensitivity to the potential due to the $\Delta v=-2$ channel closing impairs the agreement between experiment and theory for $v=48$. Below $v=43$, the rotational distributions for $\Delta v=-1$ and $\Delta v=-2$ are quite similar. Above $v=43$ the peaks of the rotational distributions for $\Delta v=-2$ move to higher values of j. These results are compatible with the theoretical conclusion that dissociation shifts from a direct mechanism to one involving intramolecular vibrational distribution in the region of the closing of the $\Delta v=-2$ channel.

The $B \leftarrow X$ rovibronic excitation spectrum of the He···Br_2 van der Waals complex was subsequently calculated using ab initio potential energy surfaces [28,35]. The coupled-cluster single double triple calculations predict double-minimum topology (linear and T-shaped wells) for the X-state potential with a low isomerization barrier. The two lowest vibrational levels, assigned to T-shaped and linear isomers using the localization patterns of the corresponding wave functions, are almost degenerated and lie slightly above the isomerization barrier. This indicated that T-shaped and linear isomers can coexist even at low temperatures and give rise to two separated bands in the excitation spectrum. The main band of the $B \leftarrow X$ excitation spectrum were thus assigned to transitions from the T-shaped isomer, whereas the very good agreement between the observed and calculated spectrum, using the ab initio X-state potential, demonstrates that the unassigned secondary band corresponds to excitation of the linear isomer of the He···Br_2(X) complex. The complete assignment of the spectrum in terms of individual rovibronic transitions was presented. In this context, He···Br_2 is the first example in which a rotational partially resolved secondary band in the spectrum has been unambiguously assigned to the linear isomer. Similar studies have been conducted for Ne···Br_2 [71,27,72,73].

Ng···ICl. Converged three-dimensional quantum mechanical calculations for photofragmentation of the He···ICl and Ne···ICl van der Waals molecule in the energy region of the electronically excited B state of ICl were conducted and compared with experiments [74,75]. Lifetimes and final state distributions for the ICl fragments were determined for vibrational predissociation from the lowest van der Waals level in the $B(v=2)$ state. Good agreement between theory and experiment was achieved using a sum of atom–atom pairwise potentials. In the case of Ne···ICl this potential energy surface predicts the equilibrium geometry of the complex to be bent at 140 degrees with the Ne atom towards the Cl end of ICl. Analysis of the quasibound wave function reveals that the highly inverted rotational distribution of the ICl fragments observed in the experiment is not due to zero-point bending motion, but to a rotational rainbow effect enhanced by the favorable initial geometry of the complex. The effect of the excitation of the bending van der Waals mode in the complex has also been studied. As compared with the lowest level, a longer lifetime and a different rotational distribution of the fragments was predicted.

The time-dependent wave packet technique has also been applied to the Golden rule treatment of vibrational predissociation in Ne···ICl [76]. The wave packet at time zero is taken as the product of the quasibound wave function and the coupling inducing predissociation. The rate for vibrational predissociation can then be obtained by Fourier transform into the energy domain of the time-dependent wave packet autocorrelation function. It was shown that when the bound-state components of the wave packet are projected out, the time-dependent version of the Golden rule approximation provides an alternative efficient technique to treat intramolecular decay.

2.2. Vibrational predissociation in the presence of IVR (intramolecular vibrational redistribution)

Unlike the distributions for He···Cl_2 and Ne···Cl_2, those of Ar···Cl_2 are complicated and strongly dependent on the initial vibrational and rotational levels [77]. For instance, excitation to $v=11$ of the B state results in $\Delta v=-2$ dissociation with enough excess energy to populate up to $j=28$ of the products. Dissociation yields a considerable excess of $j=4$, 10, 12, 22, and 28, accounting for over half the total product population. This behavior was attributed to intramolecular vibrational relaxation (IVR) involving an intermediate doorway state, and close coupling calculations confirmed this conclusion [78–80] (see Fig. 3).

Time-independent and time-dependent quantum mechanical calculations that describe the intramolecular vibrational relaxation (IVR) of Ar···Cl_2 were used to develop analytical models for this process [81]. It was shown that time-resolved experiments should reveal an oscillatory dissociation rate. These oscillations should be different for different rotational levels, and may tend to wash out if insufficient state selection is achieved in the initial excitation step. This could explain why none were observed for Ar···I_2. It was also predicted that the observed product state rotational distribution will change with the initially excited rotational state.

Several calculations were carried out to test the sensitivity of the spectroscopy and dynamics of the B state of Ar···Cl_2 to the steepness of the Morse term, α, of an atom–atom potential. In both the $\Delta v=-1$ and the $\Delta v=-2$ regimes the rate of vibrational predissociation and the product rotational distribution are extremely sensitive to the value chosen for α, but not in a regular way. For the $\Delta v=-2$ regime the variations can be attributed to spacings between resonances and the overlaps of the bright state wave functions with nearby dark states as expected from the intramolecular vibrational relaxation model. In the $\Delta v=-1$ regime, the variations are shown to originate from resonances in the $v-1$ continuum set of states. Although this makes it difficult to determine the value for α, a value of 1.8 $Å^{-1}$ is probably close to the true value.

2.3. Competition between vibrational and electronic predissociation

For many van der Waals systems in the electronic excited states, electronic predissociation can be induced by the presence of the noble gas atom and thus it will be in competition with vibrational predissociation.

2.3.1. The Ar···I_2 case

The most extensively studied dimer in this context is Ar···I_2. The first search for a fluorescence excitation spectrum of Ar···I_2

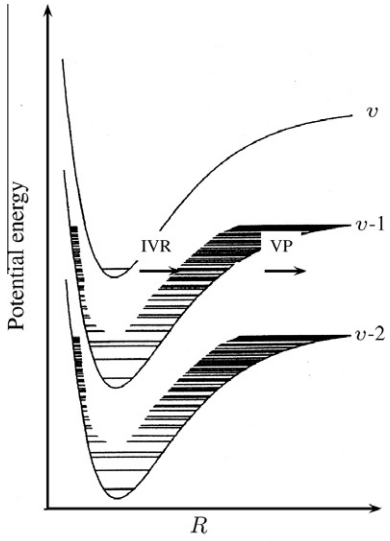

Fig. 3. The intramolecular vibrational redistribution (IVR) for the case $\Delta v = -2$. The initial quasibound level with no van der Waals excitation and v quanta in the halogen diatom, is initially formed by photon excitation. This level couples to one or more van der Waals bound states of the $v-1$ channel, which in turns couples to the continua of the $v-2$ channel.

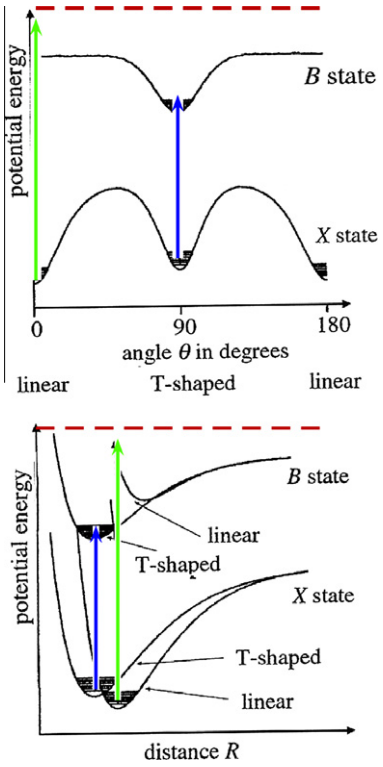

Fig. 4. The difference between excitation of a linear and a T-shaped noble gas-halogen dimer. The potential wells in the ground X and in the excited B states are very similar for the T-shaped configuration, so very little van der Waals excitation results. In contrast, there is no low energy van der Waals vibrational levels in the electronic excited state that have good Franck–Condon factors to the linear ground state.

was unsuccessful [4], and it was concluded that the spectrum was diffuse. However, 2 years later Kubiak et al. [40] found structured spectra for vibrational levels higher than $v = 11$. The intensity of the spectra oscillates with v because of a competition between vibrational and electronic predissociation. Roncero et al. [82] obtained the correct value for the electronic predissociation rate by assuming that the Ar couples the I_2 B state to the a $^3\Pi_{1g}$ state via a coupling potential that depends exponentially on the Ar-I_2 separation. The magnitude of the coupling between the two electronic states was found to be 14 cm^{-1} at the equilibrium internuclear distance. Following these first calculations, Bastida et al. [83] have used a mixed quantum classical method to simulate the competition between electronic and vibrational predissociation. They concluded that this competition causes the dissociation rate law to differ from simple first-order kinetics.

More recently [84,85], quantum dynamical calculations on the photodissociation process: $Ar\cdots I_2(X) \rightarrow Ar + I + I$ have been performed using diatomics-in-molecule semiempirical potential energy surfaces in the spectral region of the $I_2(B,\ v = 15-25) \leftarrow I_2(X,\ v = 0)$ transition. The B state responsible for vibrational predissociation producing $Ar + I_2(B)$ products is coupled to four dissociative states inducing electronic predissociation and producing $Ar + I(^2P_{3/2}) + I(^2P_{3/2})$ products. These dissociative states correspond to the a $(1g)$, a′$(0g^+)$, B″$(1u)$, $1(2g)$ electronic states of I_2. Both linear and perpendicular initial $Ar\cdots I_2(X)$ isomers were considered. For the linear isomer, only the a′ state has non-negligible effect on photodissociation dynamics: although total photon absorption cross sections are not significantly modified when coupling to a′ is taken into account, partial cross sections corresponding to vibrational predissociation are smaller (see Fig. 4). For the perpendicular isomer, resonance decay rates are increased, mainly by the coupling to a′$(0g^+)$, $1(2g)$, and a$(1g)$ states. Decay rates oscillate as a function of the vibrational excitation of $I_2(B)$ but the main source of oscillation is the intramolecular vibrational energy redistribution which occurs in vibrational predissociation, rather than Franck Condon oscillations in electronic predissociation.

2.3.2. Ng···Cl_2 dimers

For the He, Ne, and Ar···Cl_2 species in the B state, there is considerable evidence that electronic coupling takes place but no data regarding the electronic states that participate. The VP product states simply disappear for certain levels. For instance, for He···Cl_2, vibrational predissociation can be observed for levels up to $v = 23$ of the B electronic state [38]. Above this level, no signal from $Cl_2(v' < v)$ is observed. A similar phenomenon occurs at $v = 18$ for Ne···Cl_2 [59] and at $v = 13$ for Ar···Cl_2 [77]. The Ar···Cl_2 results, but not that of He···Cl_2 or Ne···Cl_2, can be attributed to a simple threshold effect. Although the thresholds for He···Cl_2 and Ne···Cl_2 occur about at the vibrational level for which $\Delta v = -1$ vibrational relaxation channel closes, vibrational predissociation should still be quite fast. For Kr···Cl_2 and Xe···Cl_2, electronic relaxation is probably faster than vibrational relaxation for all vibrational levels [86]. This is not surprising because each of these species would be expected to have strong chemical interactions in their excited electronic states. Luckily, vibrational relaxation is fast enough to compete with electronic relaxation for a few levels. This provides enough data to show that the *T-shaped* isomer is present in the supersonic expansion for both species, and product rotational distributions are observed that clearly determine the bond strengths for both molecules. Given that electronically excited Cl_2 might have been expected to undergo chemical reactions with either Kr or Xe [87], it is a little surprising that both exist as van der Waals species in the electronically excited states. Although there have been some preliminary studies of the excited-state surfaces for Xe···Cl_2 [88], this is still a wide-open problem.

Bieler et al. [89] reported more detail for the disappearance of Ne···Cl_2 vibrational predissociation product signal with increasing v and a detailed calculation of IVR and electronic predissociation (EP) dynamics for Ne···Cl_2 and Ar···Cl_2 using the best available potentials and calculated couplings between the valence electronic excited state surfaces. As in the case of Ar···I_2 discussed above, the

lack of agreement between theory and experiment is disappointing. The calculated EP rates are too slow to agree with the Ar···Cl_2 data and the EP process is too fast for lower vibrational levels of Ne···Cl_2. It would be extremely useful if the EP process could be measured directly for Ne···Cl_2, Ar···Cl_2 and Ar···I_2 rather than just inferred from disappearance of VP products.

Recently, there has finally been an example for which experiment and theory agree remarkably well regarding the competition between vibrational and electronic predissociation. Taylor et al. [90] found that the lifetime dependence on the vibrational level v for He···Br_2 and Ne···Br_2 deviates substantially from that expected from the energy gap law of Eq. (13). That the deviations were for the same vibrational levels for the two molecules supported the conclusion that electronic predissociation was the origin for the deviation. A Franck–Condon analysis suggested that the coupling was between the initially populated B state and one of the $^3\Pi_g$ states. This conclusion was supported by a wave packet calculation performed by Sanz-Sanz et al. [91]. The couplings in this case were estimated and empirically adjusted to obtain quantitative agreement with the experimental data. Later in this issue [92], Hernández Lamoneda reports on a more extensive calculation for which the valence excited electronic state couplings were calculated using ab initio techniques comparable to the previously failed study of Ne···Cl_2. The major difference between the two cases is that for Ne···Cl_2 the vibrational dynamics is in the IVR regime while for Ne···Br_2 the vibrational dynamics is in the direct vibrational predissociation regime. The success in the case of Ne···Br_2 suggests that the calculated electronic couplings are quite accurate and the main difficulty in previous studies is the quantitative calculation of IVR rates.

2.4. Photoexcitation dynamics of the linear isomers

As mentioned above, the intensive experimental study of the linear Ng···XY isomers started with the work of Burke and Klemperer [10]. Very fast, direct dissociation dynamics was inferred from the fact that the spectra were continuous. Darr and Loomis [93] showed that the dissociation dynamics of the He···ICl linear isomer results in significant vibrational cooling, but little rotational excitation, inferring a direct linear dissociation trajectory. They were also able to obtain resolved excitation spectra that break the continuum into components yielding individual product vibrational levels [94], and later [95] were able to resolve the product translational motion via ion imaging which further confirmed the direct, repulsive dissociation mechanism.

Quantum dynamical calculations on Ar···I_2 photodissociation have been performed using ab initio and semi-empirical potential energy surfaces, which support both linear and T-shaped isomers in the ground electronic state [96]. Whereas the photon absorption spectra for the T-shaped isomer consist of narrow and intense bands, those for the linear isomer result from the superposition of a continuous background and peaks due to linear quasi-bound states. Vibrational distributions for the linear isomer are broader than those originating from the T-shaped one. Rotational distributions for the linear isomer are smooth and characteristic of a fast dissociation dynamics, whereas those for the T-shaped isomer are highly oscillatory.

Pio et al. [97] were able to record the product vibrational state resolved excitation spectra for the linear isomers of the series He, Ne, and Ar···Br_2. The excitation spectra that resulted in the formation of specific product vibrational levels revealed distinct thresholds for He···Br_2 and Ne···Br_2, in each case yielding a bond energy for the linear isomer that is equal to that of the T-shaped isomer within experimental error. Interestingly the spectra for He···Br_2 peak right at the threshold energy for producing the detected product state, and gradually diminish in intensity over a range of 500 cm^{-1}. Those for Ne···Br_2 have a distinct threshold, but peak 300 cm^{-1} to the blue and gradually diminish in intensity over another range of 500 cm^{-1}. For Ar···Br_2 the thresholds are hidden by background signals from He···Br_2, and the spectra extend over a range of 1500 cm^{-1} without significantly diminishing in intensity. These spectra were qualitatively modeled using a 2-D quantum model for the coupling between the Br–Br and the Ng–Br stretching modes [97]. The conclusion from this work is that rather than consider vibrational cooling of the Br–Br stretch upon dissociation of the linear isomer, it might be more accurate to label it as direct excitation into the product continuum. Of course, this difference is somewhat semantic, but it does imply a different zero-order model for the dynamics. It would be interesting to learn whether accurate potentials can be found for the linear configuration so that dynamical calculations can achieve quantitative agreement with experiment.

3. Larger noble-gas halogen van der Waals clusters

The larger noble gas-halogen clusters provide a promising example of the transition from the small-cluster limit to model liquids. Although the ideal experiment of measuring step-by-step evaporation with both time and state resolution has yet to be performed, progress toward the goal has been made. The early work of the Levy group was mostly consistent with a single isomer for each Ng_n···I_2 cluster. They paid particular attention to the Ne_n···I_2 and found what has become known as the constant blue shift rule that they attribute to up to six Ne atoms forming a belt around the iodine waist [98]. Janda's group confirmed that tetrahedral isomers, consistent with the belt model with the two noble gas atoms in contact, exist for Ne_2···Cl_2 [99], and Ar_2···Cl_2 [100]. For He_n···Cl_2, the structure is also roughly consistent with the belt model, but in this case the He–He attraction is not strong enough to localize the He atoms within the belt [101].

The first confirmation of multiple isomers for a single $n > 1$ species was for Ar_3···Cl_2 [100]. Rotational contour analysis suggested that one of the two isomers was due to a three-atom belt, as expected, while the other was due to the Cl_2 moiety lying on top of the Ar_3 triangle. The group of Loomis built on their successful study of multiple dimer isomers by extending their techniques to the larger clusters. In analogy with the dimer species, the *belt* isomers of the larger clusters are expected to be relatively easily observable with discrete bands due to long-lived excited electronic states. By assuming that a constant band shift rule also applies to the linear configuration, Loomis et al. assigned a feature of the spectrum of He_2···Br_2 to an isomer with one helium perpendicular to the Br–Br band, and the other in the linear configuration [102]. They also identified an isomer of He_3···Br_2 with two belt and one linear He atoms, in addition to the expected 3-atom-belt isomer. Similar results were obtained for He_2···ICl and He_3···ICl [102].

That the two Ne atoms of Cl_2···Ne_2 are located perpendicular to the halogen bond was determined by rotationally resolved spectroscopy [99]. Data are also available for larger clusters involving Ne and Cl_2 [87], Br_2 [103], and ICl [55]. In contrast, no spectra have been observed for Ar_n···I_2 clusters with $n > 2$ [104]. It appears that the second Ar atom increases the electronic predissociation rate significantly above the vibrational predissociation rate. It is also possible that the presence of linear bonded isomers yield continuous, more difficult to detect spectra. This is probably due to the fact that bonding of an Ar atom anywhere other than perpendicular to the halogen bond broadens the spectra into a continuum. For He_n···I_2 clusters with $n < 4$, the main dissociation channel usually involves one quantum of I_2 vibrational energy transfer to dissociate each helium atom [98]. Because this is far more energy than necessary, it is clear that the helium atoms interact with the I_2

chromophore independently. For clusters containing Ne and Ar atoms, energy disposal is more statistical. For instance, the $Ne_6\cdots I_2$ cluster mainly dissociates via $\Delta v = -8$, less by $\Delta v = -7$, and not at all by $\Delta v = -6$ [98]. In terms of vibrational dynamics, this cluster may well be close to the statistical limit. Gutmann et al. [105] monitored the appearance of the free I_2 chromophore after excitation of $Ne_n\cdots I_2$, $n < 5$, in *real time*. The rates increase with increasing vibrational quanta, and for a given initial I_2 vibrational level, the time to dissociate all of the Ne atoms increases with the number of Ne atoms.

In the last two decades, there have been many studies of chromophore atoms and molecules embedded in large helium clusters [106]. These studies hold the tantalizing possibility of bridging the cluster-to-liquid gap for quantum liquids. $He_2\cdots Cl_2$ is the only cluster with more than one helium atom for which rotationally resolved excitation spectra and vibrational predissociation product-state distributions have been obtained [107]. Unlike the spectra of $Ne_2\cdots Cl_2$, it initially proved difficult to fit the $He_2\cdots Cl_2$ spectra with a simple structural model. This was explained by two effects [108]. Half the rotational levels are missing because of the Bose statistics of the He atoms, and there is a low-lying excited He–He vibrational level that makes important contributions to the observed spectrum. Once these effects are taken into account, the spectra can be precisely fitted, assuming additive $He\cdots Cl_2$ potentials. Much could be learned regarding the overall dissociation dynamics with vibrationally and time-resolved pump–probe dynamics studies of this and larger clusters.

Recently, Pio et al. [109] were able to directly measure the time dependence of the initially excited $Ne_2\cdots Br_2$ B state, Br_2 stretching level $16 \leqslant v \leqslant 23$; the appearance and disappearance of the $Ne\cdots Br_2$ intermediate products that had lost one or more quanta of bromine stretching vibrational energy to dissociate the first Ne atom; and the appearance of the final Br_2 product after the second Ne atom had been dissociated. For the lowest vibrational levels studied, dissociation occurred mainly via two sequential $\Delta v = -1$ steps. For higher vibrational levels, the dynamics shifted into the IVR mode and Δv values as large as -5 contributed significant probability to the product vibrational distribution. For initial $v = 21$, both $Ne\cdots Br_2$ $\Delta v = -1$ and $\Delta v = -2$ decays were observed to produce intermediates. The resulting intermediates had significantly different kinetics, with the decay rate of the $v = 20$ transient being nearly twice that of the $v = 19$ transient. Br_2 $v' = 19$ and 18 final product states were formed in almost equal amounts, but the $\Delta v = -2$ product formation rate is faster than the $\Delta v = -3$ rate. This level of detail regarding the rates for individual steps of a multistep process provides a fresh challenge to the theorists.

As the number of noble gas atoms attached to a halogen chromophore increases, the difficulty of obtaining an exact theoretical analysis increases even faster. $Ne_2\cdots Cl_2$, for instance, has six internal degrees of freedom. Although a fully quantum calculation for such a molecule may now be possible using efficient wave-packet methods, it has been achieved only once, on $Ne_2\cdots I_2$ using the multichannel time-dependent Hartree (MCTDH) methodology by Meier and Manthe [110]. Instead, recent efforts have focused on two approaches: reduced dimensionality and mixed quantum–classical analysis. Although the reduced dimensionality approach is insightful for small clusters [111–114], it leaves out those features of the *bath* that are the object of most long-term goals for cluster studies. For this reason, we concentrate here on the mixed quantum–classical approach. Considerable effort has been invested in quasi-classical analysis of noble gashalogen dynamics. The classical equations of motion are numerically solved with the initial conditions selected at random taking into account quantal distributions. To check this approximation, the first quasiclassical calculations have been conducted in $He\cdots I_2$ by Delgado-Barrio et al. [115,116]. The final rotational distribution for the I_2 fragment and the total rate for vibrational predissociation as functions of vibrational excitation were determined. Similar studies by the same group have been done for $Ne\cdots I_2$ [117,118] and $Ne\cdots Br_2$ [119]. The results demonstrated that when quantum interference effects are unimportant, the quasiclassical techniques give very good results.

García-Vela et al. [120] have focused on the clusters, such as $Ne_n\cdots I_2$, that can be compared with experiments. Although they observed that IVR increases with cluster size and other essential features of the dynamics, they concluded that the classical approach is limited by its inadequate treatment of zero-point energy effects. These are just the systems, however, for which the transfer of quanta from the halogen bond should be most *sequential*, enabling a mixed quantum–classical approach. Hernández et al. [121] proposed a combined quantum–classical approach for $He_2\cdots Cl_2$ in which the first dissociation was assumed to be classical, and the results of the trajectory calculations were used to set up initial conditions for a quantum treatment for the ejection of the second He atom. Good agreement with the data was obtained.

Subsequently, similar calculations have been done by the Delgado-Barrio's group for $Ng_n\cdots I_2$ [122,123,120,124,113,125,126]; $He\cdots I_2\cdots Ne$ [127,111,128]; $Ng_n\cdots Cl_2$ [121,129–131]; $Ng_n\cdots Br_2$ [132–134,70]; $Ng_n\cdots ICl$ [135–137].

An alternative approach is to treat the high-frequency halogen vibration as quantum while treating the noble gas atom coordinates as classical. There are two families of this approach, which vary by how the quantum and classical degrees of freedom are connected. In the mean-field approach, the classical degrees of freedom evolve on an average surface obtained from the expectation value of the potential energy operator over the wave packet describing the time evolution of the diatomic vibration. This is not appropriate for noble gas-halogen molecules because the resulting mean field potential does not mimic the true potential for the dynamics. The other approach is based on trajectory surface-hopping techniques, in which the classical degrees of freedom evolve on a potential surface corresponding to the diatomic being in one given vibrational level at each time *t*, with the possibility of transitions, *hops*, from one vibration to another. However, techniques based on surface crossing, developed for electronic transitions, are not well suited to vibrational predissociation. Instead, the molecular dynamics with quantum transitions (MDQT) method of Tully [138–140] has been successfully applied to several noble gas-halogen clusters. In this treatment, transitions between the different vibrational levels are governed by the time evolution of the wave packet describing the diatomic vibration. This is well suited for vibrational predissociation because the surfaces corresponding to different vibrational levels of the halogen are almost parallel.

For $Ne_n\cdots I_2$, $n < 6$, results based on the MDQT method nicely reproduced the final vibrational-state distribution data and the time-resolved data for the appearance of product states [141,142]. Similar good agreement between experiment and theory for the overall rate of relaxation and the final vibrational/rotational product-state distributions was obtained for $Ne_n\cdots Cl_2$ [143]. The theory allows for a more detailed analysis of the individual steps in the dynamics than are apparent from the data. Bastida et al. [143] proposed a kinetic mechanism, that involves three types of individual steps. The first two types of steps, vibrational predissociation (VP) and intramolecular vibrational redistribution (IVR), are directly analogous to the direct VP and IVR described above for the case of simple dimers. The third step, evaporative cooling (EC), occurs when energy stored in the van der Waals degrees of freedom by IVR steps *evaporates* a noble gas atom without any direct connection to the actual relaxation of the halogen. The kinetic analysis of the theoretical results showed that the probability of direct vibrational predissociation drops rapidly with increasing vibrational excitation and with

increasing numbers of Ne atoms. For instance, when $Ne_2\cdots Cl_2$ is excited to $v = 8$ of the $Cl_2(B)$ state, the ratio of direct VP to IVR followed by evaporative cooling is 0.7. For $v = 13$, the ratio drops to 0.05. For $Ne_3\cdots Cl_2$, $v = 8$, the ratio is 0.4, and direct VP disappears completely for $v = 13$. The ability to analyze data with this degree of detail is exciting for the goal of applying small-cluster insight to the overall dynamics of large clusters and, eventually, liquids. Because the MDQT technique allows the classical degrees of freedom to follow different dynamics for different vibrational channels, this allows the intermediate Δv steps to be identified. It will be especially interesting if these predictions can be compared with experimental data.

From the electronic structure point of view, studies of larger species are more complex and the difficulty in the evaluation of the PES increases with their size. Four-body systems such as $He_2\cdots Br_2(X)$ are now amenable for performing ab initio calculations with a satisfactory degree of accuracy, which then permit the testing of various models of additivity in order to describe the PES of larger $He_N\cdots Br_2(X)$ clusters. Recently, ab initio calculations at the fourth-order Møller–Plesset (MP4) and coupled-cluster [CCSD(T)] levels of theory have been performed [144] for the above mentioned tetratomic system. The surface is characterized by three minima and the minimum energy pathways through them. The global minimum corresponds to a linear He–Br_2–He configuration, and the two other ones to *police-nightstick* (one He atom in the linear configuration, and the other in the T-shaped one with respect to the bromine) and tetrahedral (with the two He atoms along a plane perpendicular to the bromine bond) structures. Analytical representations based on a sum of pairwise atom–atom interactions and a sum of three-body He–Br_2 CCSD(T) potentials [12] and He–He interaction [26,29] were checked in comparison with the tetratomic ab initio results. The sum of the three-body interactions form was found to be able to accurately represent the MP4(SDTQ)/CCSD(T) data. In order to extract information on non-additive interactions in $He_2\cdots Br_2$, equilibrium structures based on the ab initio calculations were examined [144]. By partitioning the interaction energy into components, it was found a similar nature of binding in triatomic and tetratomic complexes of such type, and thus information on intermolecular interactions available for triatomic species might serve to study larger systems. For the first time an analytical expression in accord with high level ab initio studies was proposed for describing the intermolecular interactions for such two atoms rare gas-dihalogen complexes.

Variational bound state calculation was carried out for the above surface and vdW energy levels and eigenfunctions for $J = 0$ were evaluated for $He_2\cdots Br_2$. Radial and angular distributions were calculated for the three lower vdW states and three different structural models, which correspond to linear, *police-nightstick*, and tetrahedral isomers, were determined. The binding energies and the average structures for these species have been computed. The resulting values are in excellent agreement with recent LIF experimental data available.

In later work by the Delgado-Barrio group [145], the Hartree approach was applied to get energies and density probability distributions of $Br_2(X)\cdots{}^4He_N$ clusters. The lowest energies were obtained for the value $\Lambda = 0$ of the projection of the orbital angular momentum onto the molecular axis, and the symmetric N-boson wavefunction, i.e., the Σ_g state in which all the He atoms occupy the same orbital (in contrast to the case of fermions). It stressed that both energetics and helium distributions on small clusters ($N < 18$) showed very good agreement with those obtained in *exact* DMC computations [132]. The total energy and energy per He atom changed continuously and monotonically with the cluster size, giving no indication for shell-closure effects. The energy per atom, $E(N)/N$, increased rapidly as the cluster size increased up to $N \simeq 15$ and then it slowly tended to the bulk value.

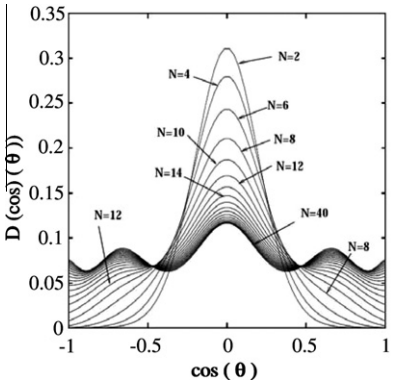

Fig. 5. Angular density distributions for the He atoms surrounding the $Br_2(X)$ molecule for different cluster sizes. (*Soruce*: adapted from [70])

In Fig. 5, Helium angular density distributions around the Br_2 molecule for different cluster sizes ($N = 2 - 40$) are displayed. Note that for the smaller clusters the angular density distributions are highly anisotropic peaking at $\pi/2$. This is a consequence of the strong anisotropy in the helium–Br_2 potential which favors the T-shape arrangement. The He atoms populate primarily the well associated with this arrangement up to about $N = 6$. For larger N, the increasing He–He repulsion causes the density distribution to flow from T-configuration well into the other potential regions. Indications for formation of two side peaks at $\pi/4$ and $3\pi/4$ are evident for $N = 12$, and these peaks are clearly present in the graphs corresponding to $N = 16$ and 18. For $N = 24$, about 4% of the He density is found at peaks adjacent to $\theta = 0$ and π. For $N \geqslant 30$, the He distributions are almost independent of the cluster size and markedly more isotropic than those for $N \leqslant 6$. This can be explained by taking into account that the strongly anisotropic potential is felt mainly by the He atoms that are close to the dopant molecule whereas the spatial clustering of the He atoms more distant from the impurity is driven primarily by the He–He interaction. This quantum chemistry-type method has an advantage over density functional theory-based techniques because it also furnishes wave-functions, which can be used to perform computations of spectra and therefore to make a better contact with the experiment. Another advantage of this approach used is that unlike the diffusion Monte Carlo method it can coherently be applied for studies of fermion and mixed bosonic/fermionic doped clusters. An example is the work on the Raman spectra of $(He)_N\cdots Br_2(X)$ clusters [146,147].

4. Ionic clusters

4.1. Historical

Historically, the fragmentation of neutral rare gas clusters upon ionization has played a crucial role in the interpretation of mass spectrometry experiments. These clusters are generated from a supersonic beam expansion in a broad distribution of sizes, then ionized and detected in a mass spectrometer. It was initially taken for granted that the size distribution obtained in the mass spectrometer reflected the neutral one. However, due to the difference in bonding nature between the neutral and ionic clusters, ionization leads to substantial internal energy excitation in the ion, which in turn leads to fragmentation. This is illustrated in Fig. 6 on the case of Ne_2, which is a typical weakly bound van der Waals dimer, while the corresponding ion is more strongly bound with a much smaller bond length and deeper well depth. Ionization being much faster than nuclear motion, it occurs for fixed positions of the nuclei ("vertical" ionization). Hence from the equilibrium bond

length of the neutral it accesses the outer part of the ionic well, which provides a lot of internal energy.

These considerations were known for some time [148–150], however, the direct proof required an experiment in which neutral cluster size could be assigned prior to ionization. This was provided by Buck and Meyer [151,152] who exploited the different kinematic behavior of different cluster sizes in a scattering experiment. The cluster beam was scattered from a helium beam, and separation was achieved by measuring angular and velocity distributions after scattering. It was shown that fragmentation was quite strong. For argon clusters up to the hexamer, the dominant fragment channel was the dimer ion Ar_2^+, and the first contribution to the Ar_3^+ ion came from Ar_5.

Despite these detailed and surprising experimental results, theoretical calculations remained sparse, due to the complexity of a realistic simulation. Because ionization corresponds to an electron abstraction from a p orbital, the molecular states of the ionic clusters are linear combinations of $3n$ atomic orbitals for the electron hole, all of which lie in the same energy region. Hence any realistic simulation would have to take into account all these electronic states and their couplings. The number of degrees of freedom makes a complete quantum simulation unfeasible. On the other hand, classical dynamics can only deal with one potential energy surface at a time. Hence the first simulations were model calculations based on physical insight gained from experiments and on what was known about dimers. For instance, Soler et al. [153] and Sáenz et al. [154] have assumed the initial formation of a dimer ion and followed the subsequent energy relaxation of the system using classical dynamics. They observed complete boiling off of small argon and xenon clusters for $n < 7$. The same conclusion was reached by Stampfli [155], who ran classical trajectories on a more realistic diatomics in molecules (DIM) description of the ground electronic state of the Ne_n^+ and Xe_n^+ clusters. The first calculation taking into account the multi-surface aspect of the ion dissociation dynamics was conducted by Kuntz and Hogreve [156] using the classical path surface hopping trajectory method. This study examined the fate of ionic clusters formed initially in the lowest three of the six A' symmetry states, and interpreted the results in terms of charge migration and non-adiabatic transitions. The first study in which all potential energy surfaces were involved used mean-field dynamics and a DIM model for the electronic Hamiltonian [157]. The monomer and dimer fragment ion proportions from Ar_3 and Ar_4 ionization were in good agreement with experiment. Other works using mean-field dynamics have appeared more recently [158,159], although so far only including small size clusters.

A systematic study of ionization-induced dissociation of neon, argon, krypton and xenon clusters was undertaken by Bonhommeau et al. [160–163] for sizes up to $n = 14$. These simulations used a variant of the molecular dynamics with quantum transitions (MDQT) of Tully [138] to describe transitions between all adiabatic potential energy surfaces involved. The electronic Hamiltonian was modeled by DIM with the addition of spin–orbit coupling and induced dipole-induced dipole interactions. The resulting fragmentation patterns are quite similar for all rare gases. Dimers are the most abundant fragments in the size range studied, with monomers as the second most important fragments for the smaller neutral cluster sizes and trimers for the larger ones. Fragmentation of the parent ions occurs in the picosecond time range, which is very fast compared to the time of flight in the detection region of a typical experiment. For the smaller cluster sizes dynamics is completed within several tens of picoseconds. For the larger cluster sizes, especially in the case of heavier rare gases, an increasing proportion of longer-lived species is appearing, in relation with the stabilization of larger fragments (trimers or higher).

In the mean time, existing experimental results were extended to larger sizes for Ar_n (up to $n = 9$) [164] and new experiments were conducted on krypton (up to $n = 7$) [165] and xenon (up to $n = 5$) clusters [163]. While the larger argon cluster sizes confirmed the good agreement between simulations and experiments, there was a surprise concerning krypton and xenon clusters. In both cases the ionic monomer is the main fragment. In the case of krypton, the sum of monomer and dimer ionic fragment proportions as a function of neutral cluster size is in very good agreement [166,165], but the experimental monomer proportion is over 90% up to $n = 7$ whereas the corresponding calculated value decreases from 50% for $n = 2$ to about 10% for $n = 7$ and reaches 0 for $n = 10$. The calculated dimer ion fragment proportion increases from 49% for $n = 2$ to a maximum of 84% for $n = 6$ and then drops again to 63% for $n = 9$, whereas the experimental values oscillate around a few %. This predominance of monomer ion fragments for the heavier rare gases remains a puzzle, although several hypotheses have been discussed [162].

Apart from the discriminating experiments cited above, in which neutral clusters were size-selected prior to ionization and therefore provided a direct comparison to simulations for the fragmentation pattern from a given initial cluster, ionic clusters have been produced in a wide range of conditions. For instance, a model based on phase space theory predicted that small Ar_2^+ and Ar_3^+ clusters could be formed in their ground electronic states and with high rotational temperatures after multiple evaporations from excited, larger clusters generated by electron or photon impact ionization of neutral species [167]. Hence there has been a lot of interest in understanding the various relaxation and dissociation mechanisms under different initial conditions for the parent ions. Argon trimer has been a subject of choice for calculations, because it is small enough that fully quantum calculations can be conducted for the ground electronic state. Buonomo et al. [168] have conducted a full quantum study on the vibrational predissociation mechanisms in Ar_3^+ ground electronic state, elaborating on an initial study by Pilar de Lara et al. [169]. Using a potential energy surface calculated by density functional methods [169], they have determined metastable states corresponding to the left hand side of the vibrational predissociation equation

$$Ar\cdots Ar_2^+(v_i = 1,2) \rightarrow Ar + Ar_2^+(v_f < v_i). \quad (16)$$

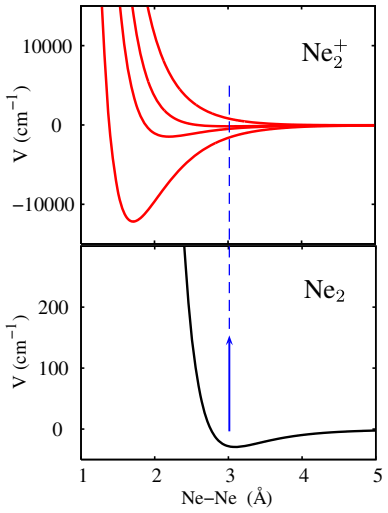

Fig. 6. Ne_2 and Ne_2^+ curves. The vertical blue arrow shows the region for vertical ionization. (For interpretation of the references to colour in this figure legend, the reader is referred to the web version of this article.)

They have obtained the corresponding lifetimes using time-independent quantum dynamics techniques for different values of the total angular momentum up to $J = 8$. It was found that lifetimes from $v_i = 2$ are shorter than the ones from $v_i = 1$, with average values of 39 ps and 50 ps for $J = 0$, respectively. Furthermore, the calculations also confirmed the tendency of the lifetimes to increase with the total angular momentum of the cluster.

5. Summary

In this review we focused on the structure and dynamics of noble gas dihalogens complexes and ionic noble gas cluster work. In some sense, these are the simplest types of problems that the Delgado Barrio group worked on in concert with many other experimental and theoretical groups around the world. These model systems help develop the language and techniques that are applied to wide variety of more complicated problems. Many such examples are given by other papers in this special issue.

References

[1] A. Rohrbacher, N. Halberstadt, K.C. Janda, Annu. Rev. Phys. Chem. 51 (2000) 405.
[2] S.J. Harris, S.E. Novick, W. Klemperer, W.E. Falconer, J. Chem. Phys. 61 (1974) 193.
[3] S.E. Novick, S.J. Harris, K.C. Janda, W. Klemperer, Can. J. Phys. 53 (1975) 2007.
[4] R.E. Smalley, D.H. Levy, L. Wharton, J. Chem. Phys. 64 (1976) 3266.
[5] J.A. Beswick, J. Jortner, Chem. Phys. Lett. 49 (1977) 13.
[6] A. Rohrbacher, J. Williams, K.C. Janda, Phys. Chem. Chem. Phys. 1 (1999) 5263.
[7] D.H. Levy, Adv. Chem. Phys. 47 (1981) 323.
[8] K.L. Saenger, G.M. McClelland, D.R. Herschbach, J. Phys. Chem. 85 (1981) 3333.
[9] J.B. Cross, J.J. Valentini, J. Chem. Phys. 77 (1982) 572.
[10] M.L. Burke, W. Klemperer, J. Chem. Phys. 98 (1993) 1797.
[11] K.C. Janda, D. Djahandideh, O. Roncero, N. Halberstadt, Chem. Phys. 239 (1998) 177.
[12] D.S. Boucher, R.A. Loomis, Adv. Chem. Phys. 138 (2008) 375.
[13] M.C. Bradke, R.A. Loomis, J. Chem. Phys. 118 (2003) 7233.
[14] D.S. Boucher, M.C. Bradke, J.P. Darr, R.A. Loomis, J. Phys. Chem. A 107 (2003) 6901.
[15] J.P. Darr, A.C. Crowther, R.A. Loomis, Chem. Phys. Lett. 378 (2003) 359.
[16] D.B. Strasfeld, J. P Darr, R.A. Loomis, Chem. Phys. Lett. 397 (2004) 116.
[17] N. Sivakumar, J.I. Cline, C.R. Bieler, K.C. Janda, Chem. Phys. Lett. 147 (1988) 561.
[18] D.G. Jahn, S.G. Clement, K.C. Janda, J. Chem. Phys. 101 (1994) 283.
[19] D.G. Jahn, W.S. Barney, J. Cabalo, S.G. Clement, T.J. Slotterback, K.C. Janda, N. Halberstadt, J. Chem. Phys. 104 (1996) 3501.
[20] D.S. Boucher, D.B. Strasfeld, R.A. Loomis, J. Chem. Phys. 123 (2005) 104312.
[21] S.E. Ray, A.B. McCoy, J.J. Glennon, J.P. Darr, E.J. Fesser, J.R. Lancaster, R.A. Loomis, J. Chem. Phys. 125 (2006) 164314.
[22] R. Prosmiti, P. Villarreal, G. Delgado-Barrio, Chem. Phys. Lett. 359 (2002) 473.
[23] R. Prosmiti, A. Valdés, P. Villarreal, G. Delgado-Barrio, J. Phys. Chem. A 108 (2004) 6065.
[24] A. Valdés, R. Prosmiti, P. Villarreal, G. Delgado-Barrio, D. Lemoine, B. Lepetit, J. Chem. Phys. 126 (2007) 244314.
[25] M.P. de Lara-Castells, R.V. Krems, A.A. Buchachenko, G. Delgado- Barrio, P. Villarreal, J. Chem. Phys. 115 (2001) 10438.
[26] R. Prosmiti, C. Cunha, P. Villarreal, G. Delgado-Barrio, J. Chem. Phys. 116 (2002) 9249.
[27] C. Cunha, R. Prosmiti, P. Villarreal, G. Delgado-Barrio, Mol. Phys. 100 (2002) 231.
[28] A.A. Buchachenko, R. Prosmiti, C. Cunha, G. Delgado-Barrio, P. Villarreal, J. Chem. Phys. 117 (2002) 6117.
[29] A. Valdés, R. Prosmiti, P. Villarreal, G. Delgado-Barrio, Mol. Phys. 102 (2004) 2277.
[30] R. Prosmiti, C. Cunha, G. Delgado-Barrio, P. Villarreal, J. Chem. Phys. 117 (2002) 7017.
[31] A. Valdés, R. Prosmiti, P. Villarreal, G. Delgado-Barrio, Chem. Phys. Lett. 375 (2003) 328.
[32] R. Prosmiti, C. Cunha, P. Villarreal, G. Delgado-Barrio, J. Chem. Phys. 119 (2003) 4216.
[33] R. Prosmiti, P. Villarreal, G. Delgado-Barrio, Israel. J. Chem. 43 (2003) x1.
[34] A. Rohrbacher, J. Williams, K.C. Janda, S.M. Cybulski, R. Burcl, M.M. Szczesniak, N. Halberstadt, J. Chem. Phys. 106 (1997) 2685.
[35] M.P. de Lara-Castells, A.A. Buchachenko, G. Delgado-Barrio, P. Villarreal, J. Chem. Phys. 120 (2004) 2182.
[36] R. Prosmiti, L. García-Gutiérrez, L. Delgado-Tellez, A. Valdés, P. Villarreal, G. Delgado-Barrio, J. Phys. 194 (2009) 122001.
[37] N. Halberstadt, J.A. Beswick, K.C. Janda, J. Chem. Phys. 87 (1987) 3966.
[38] J.I. Cline, B.P. Reid, D.D. Evard, N. Sivakumar, N. Halberstadt, K.C. Janda, J. Chem. Phys. 89 (1988) 3535.
[39] R. Prosmiti, A. Valdés, L. García-Gutierrez, L. Delgado-Tellez, P. Villarreal, G. Delgado-Barrio, AIP Conf. Proc. 1148 (2009) 334.
[40] G. Kubiak, P.S.H. Fitch, L. Wharton, D.H. Levy, J. Chem. Phys. 68 (1978) 4477.
[41] J.A. Blazy, B.M. DeKoven, T.D. Russell, D.H. Levy, J. Chem. Phys. 72 (1980) 2439.
[42] S.H. Tersigni, P. Gaspard, S.A. Rice, J. Chem. Phys. 92 (1990) 1775.
[43] J.A. Beswick, J. Jortner, J. Chem. Phys. 68 (1978) 2277.
[44] J.A. Beswick, J. Jortner, Adv. Chem. Phys. 47 (1981) 363.
[45] J.A. Beswick, G. Delgado-Barrio, J. Jortner, J. Chem. Phys. 70 (1979) 3895.
[46] G. Delgado-Barrio, J.A. Beswick, J. Chem. Phys. 73 (1980) 3653.
[47] M. Aguado, P. Villarreal, G. Delgado-Barrio, P. Mareca, J.A. Beswick, Chem. Phys. Lett. 102 (1983) 227.
[48] A.M. Cortina, S. Miret-Artés, P. Villarreal, G. Delgado-Barrio, J. Mol. Struct. 142 (1986) 513.
[49] O. Roncero, J. Campos-Martinez, A.M. Cortina, P. Villarreal, G. Delgado-Barrio, Chem. Phys. Lett. 148 (1988) 62.
[50] G. Delgado-Barrio, P. Villarreal, P. Mareca, J.A. Beswick, Int. J. Quantum Chem. 27 (1985) 173.
[51] G. Delgado-Barrio, P. Mareca, P. Villarreal, A.M. Cortina, S. Miret-Artes, J. Chem. Phys. 84 (1986) 4268.
[52] A. García-Vela, P. Villarreal, G. Delgado-Barrio, Int. J. Quantum Chem. 35 (1989) 633.
[53] A. Valdés, R. Prosmiti, P. Villarreal, G. Delgado-Barrio, H-J. Werner, J. Chem. Phys. 126 (2007) 204301.
[54] L. García-Gutierrez, L. Delgado-Tellez, A. Valdés, R. Prosmiti, P. Villarreal, G. Delgado-Barrio, J. Phys. Chem. A 113 (2009) 5754.
[55] J.M. Skene, J.C. Drobits, M.I. Lester, J. Chem. Phys. 85 (1986) 2329.
[56] J.I. Cline, N. Sivakumar, D.D. Evard, K.C. Janda, J. Chem. Phys. 86 (1987) 1636.
[57] S. Huang, C.R. Bieler, K.C. Janda, F.M. Tao, W. Klemperer, P. Casavecchia, N. Halberstadt, J. Chem. Phys. 102 (1995) 8846.
[58] J. Williams, A. Rohrbacher, J. Seong, N. Marianayagam, K.C. Janda, R. Burcl, M.M. Szczesniak, G. Chalasinski, S.M. Cybulski, N. Halberstadt, J. Chem. Phys. 111 (1999) 997.
[59] J.I. Cline, N. Sivakumar, D.D. Evard, C.R. Bieler, B.P. Reid, N. Halberstadt, S.R. Hair, K.C. Janda, J. Chem. Phys. 90 (1989) 2605.
[60] N. Halberstadt, J.A. Beswick, K.C. Janda, J. Chem. Phys. 87 (1987) 3966.
[61] P. Villarreal, G. Delgado-Barrio, J. Campos-Martínez, O. Roncero, J. Mol. Struct. (Theochem.) 166 (1988) 325.
[62] T. González-Lezana, M.I. Hernández, G. Delgado-Barrio, A.A. Buchachenko, P. Villarreal, J. Chem. Phys. 105 (1996) 7454.
[63] T. González-Lezana, M.I. Hernández, G. Delgado-Barrio, P. Villarreal, J. Chem. Phys. 106 (1997) 3216.
[64] T. González-Lezana, M.I. Hernández, G. Delgado-Barrio, A.A. Buchachenko, P. Villarreal, SPIE 3090 (1997) 118.
[65] A.A. Buchachenko, T. González-Lezana, M.I. Hernández, G. Delgado- Barrio, P. Villarreal, N.F. Stepanov, Chem. Phys. Lett. 269 (1997) 448.
[66] T. González-Lezana, M.I. Hernández, P. Villarreal, G. Delgado-Barrio, J. Mol. Struct. (Teochem.) 433 (1998) 3216.
[67] A. Rohrbacher, T. Ruchti, K.C. Janda, A.A. Buchachenko, M.I. Hernández, T. González Lezana, P. Villarreal, G. Delgado-Barrio, J. Chem. Phys. 110 (1999) 256.
[68] A.A. Buchachenko, T. González-Lezana, M.I. Hernández, M.P. de Lara-Castells, G. Delgado-Barrio, P. Villarreal, Chem. Phys. Lett. 318 (2000) 578.
[69] M.I. Hernández, T. González-Lezana, G. Delgado-Barrio, P. Villarreal, A.A. Buchachenko, J. Chem. Phys. 113 (2000) 4620.
[70] G. Delgado-Barrio, D. López-Durán, A. Valdés, R. Prosmiti, M.P. de Lara-Castells, T. González-Lezana, P. Villarreal, Progress in Theoretical Chemistry and Physics, vol. 16, Springer, 2007. 193.
[71] O. Roncero, J. Campos-Martínez, M.I. Hernández, G. Delgado-Barrio, P. Villarreal, J. Rubayo-Soneira, J. Chem. Phys. 115 (2001) 2566.
[72] R. Prosmiti, C. Cunha, A.A. Buchachenko, G. Delgado-Barrio, P. Villarreal, J. Chem. Phys. 117 (2002) 10019.
[73] T.A. Stephenson, N. Halberstadt, J. Chem. Phys. 112 (2000) 2265.
[74] R.L. Waterland, M.I. Lester, N. Halberstadt, J. Chem. Phys. 92 (1990) 4261.
[75] O. Roncero, J.A. Beswick, N. Halberstadt, P. Villarreal, G. Delgado-Barrio, J. Chem. Phys. 92 (1990) 3348.
[76] P. Villarreal, S. Miret-Artés, O. Roncero, G. Delgado-Barrio, J.A. Beswick, N. Halberstadt, R.D. Coalson, J. Chem. Phys. 94 (1991) 4230.
[77] D.D. Evard, C.R. Bieler, J.I. Cline, N. Sivakumar, K.C. Janda, J. Chem. Phys. 89 (1988) 2829.
[78] K.C. Janda, O. Roncero, N. Halberstadt, J. Chem. Phys. 105 (1996) 5830.
[79] N. Halberstadt, J.A. Beswick, O. Roncero, K.C. Janda, J. Chem. Phys. 96 (1992) 2404.
[80] N. Halberstadt, S. Serna, O. Roncero, K.C. Janda, J. Chem. Phys. 97 (1992) 341.
[81] O. Roncero, P. Villarreal, G. Delgado-Barrio, N. Halberstadt, K.C. Janda, J. Chem. Phys. 99 (1993) 1035.
[82] O. Roncero, N. Halberstadt, J.A. Beswick, J. Chem. Phys. 104 (1996) 7554.
[83] A. Bastida, J. Zuniga, A. Requena, N. Halberstadt, J.A. Beswick, Chem. Phys. 240 (1999) 229.
[84] B. Lepetit, O. Roncero, A.A. Buchachenko, N. Halberstadt, J. Chem. Phys. 116 (2002) 8367.
[85] A.A. Buchachenko, N. Halberstadt, B. Lepetit, O. Roncero, Int. Rev. Phys. Chem. 22 (2003) 153.
[86] C.R. Bieler, K.E. Spence, K.C. Janda, J. Phys. Chem. 95 (1991) 5058.

[87] M. Boivineau, J. Le Calvé, M.C. Castex, C. Jouvet, Chem. Phys. Lett. 130 (1986) 208.
[88] D.M. Proserpio, R. Hoffman, K.C. Janda, J. Am. Chem. Soc. 113 (1991) 7148.
[89] C.R. Bieler, K.C. Janda, R Hernández Lamoneda, O. Roncero, J. Phys. Chem. A 114 (2010) 3050.
[90] M.A. Taylor, J.M. Pio, W.E. van der Veer, K.C. Janda, J. Chem. Phys. 132 (2010) 104309.
[91] C. Sanz-Sanz, O. Roncero, R. Hernández Lamoneda, J.M. Pio, M.A. Taylor, K.C. Janda, J. Chem. Phys. 132 (2010) 221103.
[92] R. Hernández Lamoneda, C. Sanz-Sanz, O. Roncero, J.M. Pio, M.A. Taylor, K.C. Janda, Chem. Phys., this issue, 2011.
[93] J.P. Darr, R.A. Loomis, Faraday Discuss. 127 (2004) 2677.
[94] J.P. Darr, J.J. Glennon, R.A. Loomis, J. Chem. Phys. 122 (2005) 131101.
[95] Y. Zhang, K. Vidma, D.H. Parker, R.A. Loomis, J. Chem. Phys. 130 (2009) 104302.
[96] O. Roncero, B. Lepetit, J.A. Beswick, N. Halberstadt, A.A. Buchachenko, J. Chem. Phys. 115 (2001) 6961.
[97] J.M. Pio, W.E. van der Veer, C.R. Bieler, K.C. Janda, J. Chem. Phys. 128 (2008) 134311.
[98] J.E. Kenny, K. E Johnson, W. Sharfin, D.H. Levy, J. Chem. Phys. 72 (1980) 1109.
[99] S.R. Hair, J.I. Cline, C.R. Bieler, K.C. Janda, J. Chem. Phys. 90 (1989) 2935.
[100] C.R. Bieler, D.D. Evard, K.C. Janda, J. Phys. Chem. 94 (1990) 7452.
[101] M.I. Hernández, N. Halberstadt, W.D. Sands, K.C. Janda, J. Chem. Phys. 113 (2000) 7252.
[102] J.P. Darr, R.A. Loomis, A.B. McKoy, J. Chem. Phys. 122 (2005) 044318.
[103] B.A. Swartz, D.E. Brinza, C.M. Western, K.C. Janda, J. Phys. Chem. 88 (1984) 6272.
[104] K.E. Johnson, W. Sharfin, D.H. Levy, J. Chem. Phys. 74 (1981) 163.
[105] M. Gutman, D.M. Willberg, A.H. Zewail, J. Chem. Phys. 97 (1992) 8048.
[106] J.P. Toennies, A.F. Vilesov, Annu. Rev. Phys. Chem. 49 (1998) 1.
[107] W.D. Sands, C.R. Bieler, K.C. Janda, J. Chem. Phys. 95 (1991) 729.
[108] M.I. Hernández, N. Halberstadt, J. Chem. Phys. 100 (1994) 7828.
[109] J.M. Pio, M.A. Taylor, W.E. van der Veer, C.R. Bieler, J.A. Cabrera, K.C. Janda, J. Chem. Phys. 133 (2010) 014305.
[110] C. Meier, U. Manthe, J. Chem. Phys. 115 (2001) 5477.
[111] P. Villarreal, A. Varadé, G. Delgado-Barrio, J. Chem. Phys. 90 (1989) 2684.
[112] P. Villarreal, S. Miret-Artés, O. Roncero, S. Serna, J. Campos- Martínez, G. Delgado-Barrio, J. Chem. Phys. 93 (1990) 4016.
[113] O. Roncero, G. Delgado-Barrio, M.I. Hernández, J. Campos-Martínez, P. Villarreal, Chem. Phys. Lett. 246 (1995) 187.
[114] F. Le Quéré, S.K. Gray, J. Chem. Phys. 98 (1993) 5396.
[115] G. Delgado-Barrio, P. Villarreal, P. Mareca, G. Albeda, J. Chem. Phys. 78 (1983) 280.
[116] P. Villarreal, G. Delgado-Barrio, P. Mareca, J.A. Beswick, J. Mol. Struct. Theochem 120 (1985) 303.
[117] G. Delgado-Barrio, P. Villarreal, P. Mareca, J.A. Beswick, J. Comput. Chem. 5 (1984) 322.
[118] J. Rubayo-Soneira, A. Garcí a-Vela, G. Delgado-Barrio, P. Villarreal, Chem. Phys. Lett. 243 (1995) 236.
[119] R. Prosmiti, P. Villarreal, G. Delgado-Barrio, O. Roncero, Chem. Phys. Lett. 359 (2002) 229.
[120] A. Garcí a-Vela, P. Villarreal, G. Delgado-Barrio, J. Chem. Phys. 94 (1991) 7868.
[121] M.I. Hernández, A. Garcí a-Vela, C. Garcí a-Rizo, N. Halberstadt, P. Villarreal, G. Delgado-Barrio, J. Chem. Phys. 108 (1998) 1989.
[122] A. Garcí a-Vela, P. Villarreal, G. Delgado-Barrio, J. Chem. Phys. 92 (1990) 6504.
[123] A. Garcí a-Vela, P. Villarreal, G. Delgado-Barrio, J. Mol. Struct. 210 (1990) 237.
[124] J. Campos-Martínez, M.I. Hernández, O. Roncero, P. Villarreal, G. Delgado-Barrio, Chem. Phys. Lett. 246 (1995) 197.
[125] A. García-Vela, J. Rubayo-Soneira, G. Delgado-Barrio, P. Villarreal, J. Chem. Phys. 104 (1996) 8405.
[126] E. Carmona-Novillo, J. Campos-Martínez, M.I. Hernández, O. Roncero, P. Villarreal, G. Delgado-Barrio, Mol. Phys. 98 (2000) 1783.
[127] N. Martín, G. Delgado-Barrio, P. Villarreal, P. Mareca, S. Miret-Artes, J. Mol. Struct. 142 (1986) 501.
[128] A. Garcí a-Vela, P. Villarreal, G. Delgado-Barrio, J. Chem. Phys. 92 (1990) 496.
[129] C. García-Rizo, M.I. Hernández, A. García-Vela, P. Villarreal, G. Delgado-Barrio, J. Mol. Struct. (Theochem.) 493 (1999) 125.
[130] M.P. de Lara-Castells, P. Villarreal, G. Delgado-Barrio, A.O. Mitrushchenkov, J. Chem. Phys. 131 (2009) 194101.
[131] R. Prosmiti, O. Roncero, G. Delgado-Barrio, F.A. Gianturco, J. Jellinek, P. Villarreal, in: AIP Conf. Proc., in press.
[132] C. Di Paola, F.A. Gianturco, D. López-Durán, M.P. de Lara-Castells, G. Delgado-Barrio, P. Villarreal, J. Jellinek, Chem. Phys. Chem. 6 (2005) 1348.
[133] O. Roncero, R. Pérez de Tudela, M.P. de Lara-Castells, R. Prosmiti, G. Delgado-Barrio, P. Villarreal, Int. J. Quantum Chem. 107 (2007) 2756.
[134] M.P. de Lara-Castells, P. Villarreal, G. Delgado-Barrio, A.O. Mitrushchenkov, Int. J. Quantum Chem. 111 (2011) 406.
[135] A. Valdés, R. Prosmiti, P. Villarreal, G. Delgado-Barrio, J. Chem. Phys. 125 (2006) 014313.
[136] M.P. de Lara-Castells, R. Prosmiti, G. Delgado-Barrio, D. López- Durán, P. Villarreal, F.A. Gianturco, J. Jellinek, Phys. Rev. A 74 (2006) 054611.
[137] M.P. de Lara-Castells, R. Prosmiti, D. López-Durán, G. Delgado- Barrio, P. Villarreal, F.A. Gianturco, J. Jellinek, Phys. Scrip. 76 (2007) C96.
[138] J.C. Tully, J. Chem. Phys. 93 (1990) 1061.
[139] J.C. Tully, Int. J. Quantum Chem. 40 (1991) 299.
[140] J. Tully, in: D. Thompson (Ed.), Modern Methods for Multidimensional Dynamics Computations in Chemistry, World Sci., 1998, p. 34.
[141] A. Bastida, J. Zuniga, A. Requena, N. Halberstadt, J.A. Beswick, J. Chem. Phys. 109 (1998) 6320.
[142] S. Fernandez-Alberti, N. Halberstadt, J.A. Beswick, A. Bastida, J. Zuniga, A. Requena, J. Chem. Phys. 111 (1999) 239.
[143] A. Bastida, B. Miguel, J. Zuniga, A. Requena, N. Halberstadt, J.A. Beswick, J. Chem. Phys. 111 (1999) 111.
[144] Alvaro Valdés, R. Prosmiti, P. Villarreal, G. Delgado-Barrio, J. Chem. Phys. 122 (2005) 044305.
[145] M.P. de Lara-Castells, D. López-Durán, G. Delgado-Barrio, P. Villarreal, C. Di Paola, F.A. Gianturco, J. Jellinek, Phys. Rev. A 71 (2005) 033203.
[146] D. López-Durán, M.P. de Lara-Castells, G. Delgado-Barrio, P. Villarreal, C. Di. Paola, F.A. Gianturco, J. Jellinek, J. Chem. Phys. 121 (2004) 2975.
[147] D. López-Durán, M.P. de Lara-Castells, G. Delgado-Barrio, P. Villarreal, C. Di. Paola, F.A. Gianturco, J. Jellinek, Phys. Rev. Lett. 93 (2004) 053401.
[148] K. Stephan, T.D. Märk, Chem. Phys. Lett. 90 (1982) 51.
[149] D.R. Worsnop, S.J. Buelow, D.R. Herschbach, J. Phys. Chem. 88 (1984) 4506.
[150] H. Haberland, Surf. Sci. 156 (1985) 305.
[151] U. Buck, H. Meyer, Phys. Rev. Lett. 52 (1984) 109.
[152] U. Buck, H. Meyer, J. Chem. Phys. 84 (1986) 4854.
[153] J.M. Soler, J.J. Sáenz, N. García, O. Echt, Chem. Phys. Lett. 109 (1984) 71.
[154] J.J. Sáenz, J.M. Soler, N. García, Surf. Sci. 156 (1985) 121.
[155] P. Stampfli, Z. Phys. D 40 (1997) 345.
[156] P.J. Kuntz, J.J. Hogreve, J. Chem. Phys. 95 (1991) 156.
[157] A. Bastida, N. Halberstadt, J.A. Beswick, F.X. Gadea, U. Buck, R. Galonska, C. Lauenstein, Chem. Phys. Lett. 249 (1996) 1.
[158] D. Hrivňák, R. Kalus, F.X. Gadéa, Europhys. Lett. 71 (2005) 42.
[159] I. Janeček, D. Hrivňák, R. Kalus, F.X. Gadéa, J. Chem. Phys. 125 (2006) 104315.
[160] D. Bonhommeau, A. Viel, N. Halberstadt, J. Chem. Phys. 123 (2005) 54316.
[161] D. Bonhommeau, N. Halberstadt, A. Viel, J. Chem. Phys. 124 (2006) 184314.
[162] D. Bonhommeau, T. Bouissou, N. Halberstadt, A. Viel, J. Chem. Phys. 124 (2006) 164308.
[163] V. Poterya, M. Fárník, U. Buck, D. Bonhommeau, N. Halberstadt, Int. J. Mass Spectrom. 280 (2009) 78.
[164] P. Lohbrandt, R. Galonska, H. Kim, M. Schmidt, C. Lauenstein, U. Buck, in: R. Campargue (Ed.), Atomic and Molecular Beams: The State of the Art 2000, Springer-Verlag, Berlin Heidelberg, 2001, p. 623.
[165] C. Steinbach, M. Fárník, U. Buck, C.A. Brindle, K.C. Janda, J. Phys. Chem. A 110 (2006) 9108.
[166] D. Bonhommeau, N. Halberstadt, U. Buck, Int. Rev. Phys. Chem. 26 (2007) 353.
[167] A.J. Stace, J. Chem. Phys. 93 (1990) 6502.
[168] E. Buonomo, F.A. Gianturco, M.P. de Lara, G. Delgado-Barrio, S. Miret-Artés, P. Villarreal, Chem. Phys. 218 (1997) 71.
[169] M. Pilar de Lara, P. Villarreal, G. Delgado-Barrio, S. Miret-Artés, E. Buonomo, F.A. Gianturco, Chem. Phys. Lett. 242 (1995) 336.

J.A. Beswick after a Ph.D. in molecular photophysics at the University of Paris, J. Alberto Beswick started working on van der Waals molecules in collaboration with Joshua Jortner at the University of Tel-Aviv. Returning to France he held a position at the CNRS and then at the University of Orsay as Professor of Physics. Since 1995 he moved to the University of Toulouse.

Nadine Halberstadt started studying energy transfer and dissociation of Van der Waals dimers during her Ph.D. at Paris XI (Orsay) University. She went on to study noble gas halogen and polyatomic complexes during her postdoc in Pittsburgh with Janda in 1987, and the first part of her career as a CNRS researcher at the Photophysique Moléculaire Laboratory in Orsay. She then moved to the University of Toulouse in 1994, where she extended the number of noble gas atoms included in the Van der Waals complexes, and started studying the fragmentation of ionized noble gas clusters. Her current research interests are centered on the theoretical description of the influence of the environment (quantum clusters, clathrates, ice) on molecular dissociative processes.

Kenneth Janda started to study noble gas-halogen van der Waals dimers during his Ph.D. studies with William Klemperer at Harvard University. His work in the field has concentrated on pump-probe studies to determine structure, lifetimes, product state distributions and branching ratios for species containing chlorine and bromine. He was lucky enough to meet Gerardo Delgado Barrio, as well as the coauthors of this review, early in his career and has had many fruitful collaborations with each of them, as well as other members of the Madrid group. Other fields of research have included scattering of noble gas atoms from surfaces, mass spectrometry of doped helium clusters and formation kinetics and spectroscopy of gas hydrate clathrates. He is currently Professor of Chemistry and Dean of Physical Sciences at the University of California, Irvine.